Polymer 51 (2010) 2636–2642

Contents lists available at ScienceDirect

Polymer

journal homepage: www.elsevier.com/locate/polymer

Fouling release nanostructured coatings based on PDMS-polyurea segmented copolymers

Jason Fang [a], Antonios Kelarakis [a], Dongyan Wang [a], Emmanuel P. Giannelis [a,*], John A. Finlay [b], Maureen E. Callow [b], James A. Callow [b]

[a] Department of Materials Science and Engineering, Cornell University, Bard Hall, Ithaca, New York, NY 14853, USA
[b] School of Biosciences, University of Birmingham, Birmingham B15 2TT, UK

ARTICLE INFO

Article history:
Received 22 January 2010
Accepted 10 April 2010
Available online 18 April 2010

Keywords:
Nanostructuring
Fouling release
Surface topology

ABSTRACT

The bulk and surface characteristics of a series of coatings based on PDMS-polyurea segmented copolymers were correlated to their fouling release performance. Incorporation of polyurea segments to PDMS backbone gives rise to phase separation with the extensively hydrogen bonded hard domains creating an interconnected network that imparts mechanical rigidity. Increasing the compositional complexity of the system by including fluorinated or POSS-functionalized chain extenders or through nanoclay intercalation, confers further thermomechanical improvements. In analogy to the bulk morphology, the surface topography also reflects the compositional complexity of the materials, displaying a wide range of motifs. Investigations on settlement and subsequent removal of *Ulva* sporelings on those nanostructured surfaces indicate that the work required to remove the microorganisms is significantly lower compared to coatings based on standard PDMS homopolymer. All in all, the series of materials considered in this study demonstrate advanced fouling release properties, while exhibiting superior mechanical properties and, thus, long term durability.

© 2010 Elsevier Ltd. All rights reserved.

1. Introduction

The colonization of immersed surfaces by a community of organisms, termed fouling, is considered a major operating problem for the shipping and aquaculture industries [1–3]. Biofilm formation on marine vessels leads to reduced speed and carrying capacity, resulting in increased propulsive power and fuel consumption, and at the same time accelerating corrosion [4–6]. Suffice to say that a substantial amount of time and money is needed to combat fouling, given that remedial strategies require high maintenance cost.

The recruitment and growth of fouling species strongly depends on several external parameters such as temperature, hydrostatic pressure, water salinity and the availability of nutrients. The great diversity of organisms means that for effective control antifouling agents with multilevel functionalities are required. For a while, self-polishing coatings which release toxic tributyltin (TBT) appeared to be an ideal solution, but due to the toxicity of TBT and its persistence in the environment its use is now globally prohibited [7,8]. Some antifouling paints, although effective, containing copper and a range of organic biocides also have detrimental environmental impact and their use in the future may also be restricted [9]. Therefore, there still exists a need to develop non-toxic, environmentally friendly antifouling coatings [10].

To this end, two main approaches have been utilized; antifouling i.e. technologies that inhibit the settlement of fouling organisms and fouling release coatings that 'release' accumulated fouling hydrodynamically [11,12]. The ideal coating system involves a tough, non-toxic, polymer that combines the appropriate surface characteristics necessary to retard settlement and/or the adhesion of fouling organisms such as low surface energy, low surface roughness, low porosity and high molecular mobility. In addition, chemical and physical stability in seawater, appropriate film-forming characteristics, and good adhesion to a variety of hull materials are desirable properties. Such a material would act in two ways: by inhibiting settlement i.e. attachment of the colonizing stages (antifouling, AF), and/or by weakening their adhesion strength (fouling release, FR). In the latter case, organisms that do stick can be easily removed hydrodynamically, ideally by simply bringing the ship to speed.

Silicones based on polydimethylsiloxane (PDMS) represent the only class of polymers currently used in commercial fouling release

* Corresponding author.
E-mail address: epg2@cornell.edu (E.P. Giannelis).

0032-3861/$ – see front matter © 2010 Elsevier Ltd. All rights reserved.
doi:10.1016/j.polymer.2010.04.024

coatings. The properties which make them suited for this purpose are their inherently low values of glass transition temperature (T_g), surface energy, and elastic modulus, combined with good chemical stability and ease of film formation. On the other hand, neat silicones display exceptionally poor mechanical properties (raising concerns about their long term durability), and are therefore typically reinforced with large quantities of inorganic particles or by chemical cross-linking. However, such strategies have detrimental effects on toughness, processability, and chain mobility, which, in turn, adversely affect fouling release behavior [13,14].

Recent advances in fouling release coatings underscore the critical role of topographical and roughness characteristics to the detachment stress of soft and hard foulants [15–18]. Architectural control of the surface features can take place through compositional induced phase separation within the polymer [19–21], and/or by introducing highly anisotropic nanoadditives [22,23].

In this study we report on a series of non-toxic nanostructured coatings based on PDMS-polyurea segmented copolymers that exhibit high level of mechanical strength coupled with enhanced fouling release characteristics. Surfaces with both nanoscopically and microscopically resolved topographical features were generated by varying the hard segment content, by using fluorinated and POSS-functionalized chain extenders, or by clay intercalation. The physical and surface characteristics of the segmented copolymers and their nanohybrid analogues were correlated to their fouling release performance.

2. Experimental section

2.1. Materials

PDMS-polyurea segmented copolymers (A12M, A15M, A32M) were synthesized following a one-step synthetic approach instead of the two-step route described previously [24]. The synthesis (Scheme 1) is based on polycondensation of PDMS-diamine and 4,4-methylenebis phenyl isocyanate (MDI). PDMS-diamines with different molecular weight were reacted with the appropriate amount of MDI (Table 1) in order to synthesize a series of copolymers with varying amounts of hard/soft segments. Specifically a round-bottom flask with magnetic spin bar was vented and filled with nitrogen. 1 g of MDI (Oekanal) was first dissolved into 38 ml THF and then poured into the flask. Another solution was prepared separately by dissolving the appropriate amount of the PDMS-diamine (Gelest) in 62 ml THF and added slowly to the flask (~1 h). The solution was left for six more hours to complete polymerization under nitrogen flow at room temperature, while the progress of reaction was monitored by FTIR spectroscopy. Afterwards, the solution was poured into a Teflon mold and allowed to dry overnight before being placed in a vacuum oven at 80 °C for 10 h.

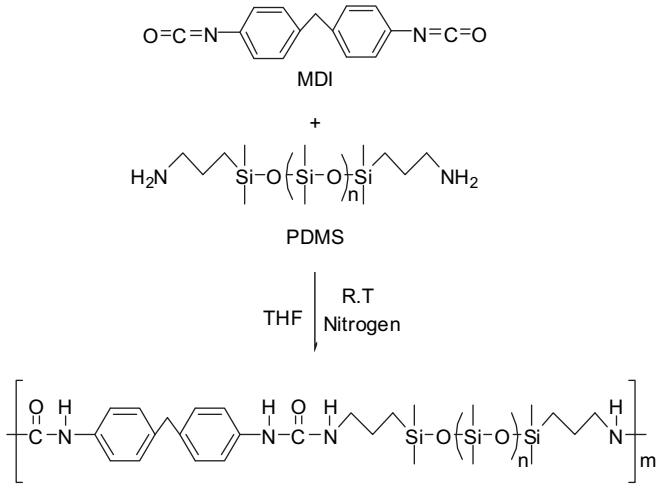

Scheme 1. Reaction scheme for the synthesis of PDMS-polyurea segmented copolymers.

Table 1
Reactants used for the synthesis of PDMS-polyurea segmented copolymers.

Copolymer	PDMS M_w (g/mol)	Weight ratio PDMS/MDI
A12M	1000	80/20
A15M	3000	92/8
A32M	30000	99/1

Fluorinated PDMS-polyurea segmented copolymers (A12MF). The fluorinated segmented copolymer (A12MF) was prepared following the same protocol described above (PDMS $M_w = 1000$ g/mol) except that 4,4′-Diaminooctafluorobiphenyl (F8) (Aldrich) was also used in addition to MDI (molar ratio PDMS-amine:F8 = 1:1). The mixture of three components was left for 20 h to react and then treated as described above (Scheme 2).

POSS-functionalized PDMS-polyurea segmented copolymer (A12MPOSS). Aminoethylaminopropylisobutyl polyhedral oligomeric silsesquioxane (POSS) (Gelest) with $M_W = 917.65$ g/mol, was included as the third reactant (PDMS $M_w = 1000$ g/mol) (Scheme 3).

PDMS-polyurea segmented copolymer/clay hybrid (A12M/clay). Sodium montmorillonite clay (Southern Clay Products) was first ion exchanged with a protonated amine terminated PDMS ($M_w = 30{,}000$ g/mol) before adding to the reactant solution. The concentration of the organically modified clay to the resulting composite was 10 wt% in A12M polymer matrix.

The nomenclature of the various materials used in this study, together with a brief description of their compositional characteristics is listed in Table 2.

2.2. Methods

Dynamic Mechanic Analysis (DMA) was performed in tensile mode using a DMA 2980 from TA instruments. 30×6 mm^2 rectangular shape, free standing samples were cast from solution. Spectra were taken from −130 to 100 °C at a single frequency (1 Hz).

Tensile tests were performed on an Instron 5800 Series controller equipped with a 5 kN load cell at a constant strain rate 5 mm/min. Dog-bone shape specimens were cast from solution. Every set of samples was measured five times for accuracy.

X-ray photoelectron spectroscopy (XPS) was performed on a Surface Science Instrument SSX-100 UHV system.

Dynamic Contact Angle (DCA) measurements were made on a Cahn Radian DCA analyzer using a fixed, transfer speed of 24 μm/s. Specimens consisted of free standing films cut into 1×3 cm^2 rectangles.

Surface topography was characterized with a MicroXAM interferometric Surface Profiler from ADE Phase Shift using the optical non-contact mode. The technique provides a 1 nm vertical and 500 nm lateral resolution, respectively.

Scanning Electronic Microscopy (SEM) images were obtained on a Keck Field Emission Scanning Electron Microscope (FE-SEM), LEO 1550. The spatial resolution is 1 nm at 20 keV and 2.5 nm at 5 keV, respectively.

2.3. Biofouling testing

(1) **Settlement of Ulva spores**. Substrates were prepared by spray coating on glass slides covered with a tie-layer. Spore density

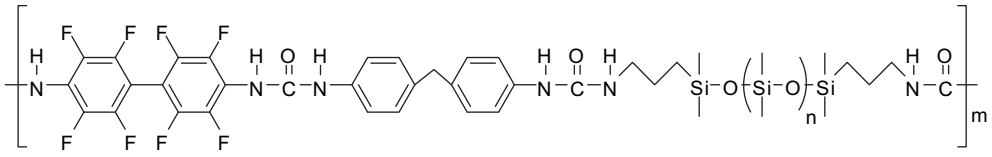

Scheme 2. Molecular architecture of A12MF.

was assessed by cell counts on fixed slides using a fluorescence microscope to visualize cells and image analysis software for counting. Sporelings of *Ulva* (young plants) were grown for 7 days. Sporeling biomass was quantified by measurement of the in-situ fluorescence of chlorophyll in a Tecan fluorescence plate reader. Fluorescence was recorded as Relative Fluorescence Units (RFU). Silastic^{R}-T2 used as standard was purchased from Dow Corning.

(2) **Attachment strength of Ulva sporelings**. The strength of attachment of the sporelings was assessed using a water jet. Each of the six replicate slides was subjected to a single applied pressure. A series of water pressures were used and the proportion of biomass removed determined using the fluorescence plate reader (initial biomass − remaining biomass = biomass removed).

3. Results and discussion

3.1. Mechanical properties

It is well established that segmented copolymers can undergo microphase separation into soft and hard domains giving rise to hierarchically ordered structures that display a wide range of morphologies [25–27]. This type of self-organization is thermodynamically driven (unfavorable enthalpic contribution of intersegmental mixing) with hydrogen bonding diminishing (hard-hard bridging) or even enhancing (hard-soft bridging) the compatibility of the two phases. The nanoscale features of the assemblies are governed by a number of architectural parameters such as chemical composition, block length and sequence and volume fraction of the components. The extent of phase segregation plays a dual role to the fouling release performance of an elastomeric coating by dictating the physical (bulk) properties as well as its surface characteristics.

In particular, the mechanical properties of segmented copolymers critically depend upon the hard segment content (HSC) and the geometry of the hard domains [28–30]. This is a direct consequence of the fact that hard domains act as physical crosslinks within the polymer matrix enabling a self-reinforcing mechanism. At high HSC values a percolated, three dimensional network of rigid domains can be formed. The tensile curves of segmented copolymers A12M, A15M and A32M with HSC 20, 8 and 1 wt%, respectively are shown in Fig. 1. The stress–strain plots reveal the elastomeric nature of the copolymers due to the flexibility of PDMS component. Both elastic modulus and ultimate strength increase by several orders of magnitude with HSC, at the expense of elongation at failure, so that only A32M follows typical rubber like deformation.

The DMA profiles of six different materials considered in this study are shown in Fig. 2. All systems show a glass transition of the soft segments centered at approximately −110 °C (T_g^S). This value appears to be relatively insensitive to compositional variables, an effect generic to this type of systems [24]. An additional, much more intense, transition was observed only for A32M at −50 °C and is accompanied by a dramatic drop of storage modulus by four orders of magnitude. On the basis of DSC thermographs (data not shown here) this transition can be ascribed to the melting point of PDMS crystals (T_m) [31]. Besides A32M, all other materials exhibit an extended rubbery zone above T_g^S. The high plateau modulus and its weak temperature dependence indicate the development of a well interconnected, extensively hydrogen bonded network of the hard segments. Note that at room temperature the elastic modulus of A12M (HSC = 20 wt%) is 86 MPa compared to less than 0.4 MPa for A32M (HSC = 1 wt%).

Incorporation of fluorinated chain extenders (A12MF) results in a two-fold increase of the storage modulus within the glassy zone and a seven-fold increase at room temperature, compared to the non-fluorinated analogue, A12M. These results suggest that the presence of fluorinated groups further promotes microphase separation, thus providing a more effective self-reinforcing mechanism [32].

Clay platelets can be viewed as secondary cross-linkers (although functioning in a very different length scale compared to hard polymer segments) contributing to the long-range connectivity of the hard segments. At the same time, clay nanolayers can confer mechanical strength in keeping with general trends established for clay nanocomposites. In principle, the strength of organic–inorganic interactions greatly affects the level of nanoclay dispersion, the load transfer efficiency and, ultimately, the mechanical response of the hybrids [33,34]. A possibility unique for thermoplastic elastomers is the selective localization of the clay

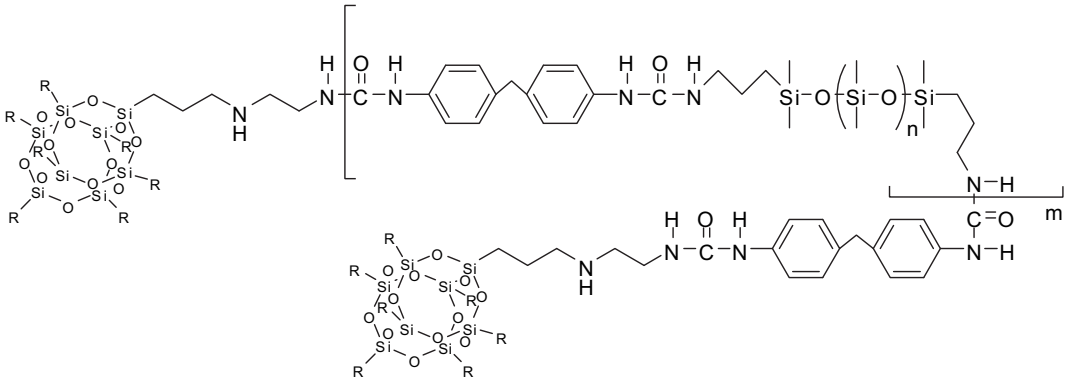

Scheme 3. Molecular architecture of A12MPOSS.

Table 2
Nomenclature, brief description and compositional characteristics of the materials.

Copolymers	Description	Composition (molar ratio)
A12M	Segmented copolymer	PDMS:MDI = 1:1 (PDMS, M_w = 1000 g/mol)
A15M	Segmented copolymer	PDMS:MDI = 1:1 (PDMS, M_w = 3000 g/mol)
A32M	Pure copolymer	PDMS:MDI = 1:1 (PDMS, M_w = 30000 g/mol)
A12MF	Fluorinated segmented copolymer	PDMS:MDI:F8 = 1:2:1
A12MPOSS	POSS-functionalized segmented copolymer	PDMS:MDI = 1:1, 38 wt% POSS
A12M/clay	Clay nanocomposite based on A12M	PDMS:MDI = 1:1, 10 wt% clay

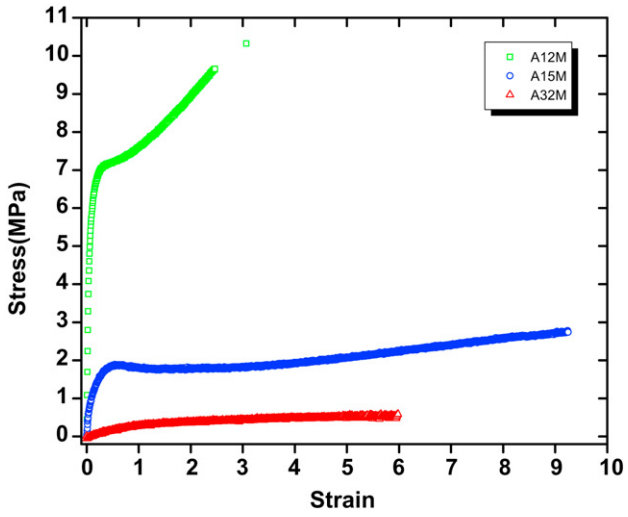

Fig. 1. Stress–strain curves of PDMS-polyurea segmented copolymers with various hard segment content.

nanoparticles to either the soft or the hard segments, although this behavior is subject to a very specific processing protocol [35]. The higher storage modulus of A12M/clay (Fig. 2) is consistent with a high level of polymer intercalation within the clay galleries and suggests the presence of favorable guest/host interactions.

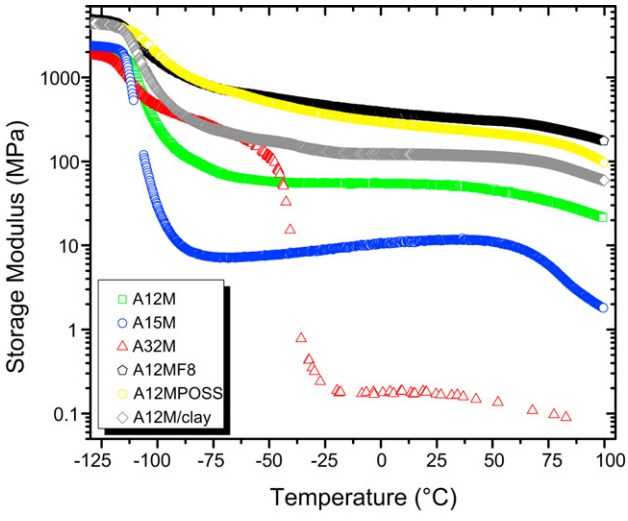

Fig. 2. DMA spectra of various systems based on PDMS-polyurea segmented copolymers.

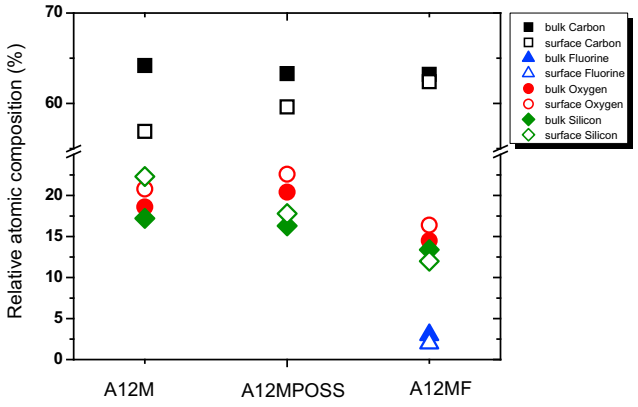

Fig. 3. Surface elemental composition (open symbols) determined by XPS measurements compared to the calculated stoichiometric values (filled symbols) for a series of copolymers.

Finally the storage modulus of A12MPOSS is higher than that of A12M within the entire temperature window considered (Fig. 2). The higher modulus is consistent with results showing that POSS nanoparticles covalently attached to macromolecular chains can effectively alter the local and global dynamics of the macromolecular chains, imparting substantial mechanical reinforcement [36].

3.2. Surface characterization

It has been long realized that bioadhesion in a surface is dictated by the interplay of wettability and topography [16,18]. Therefore,

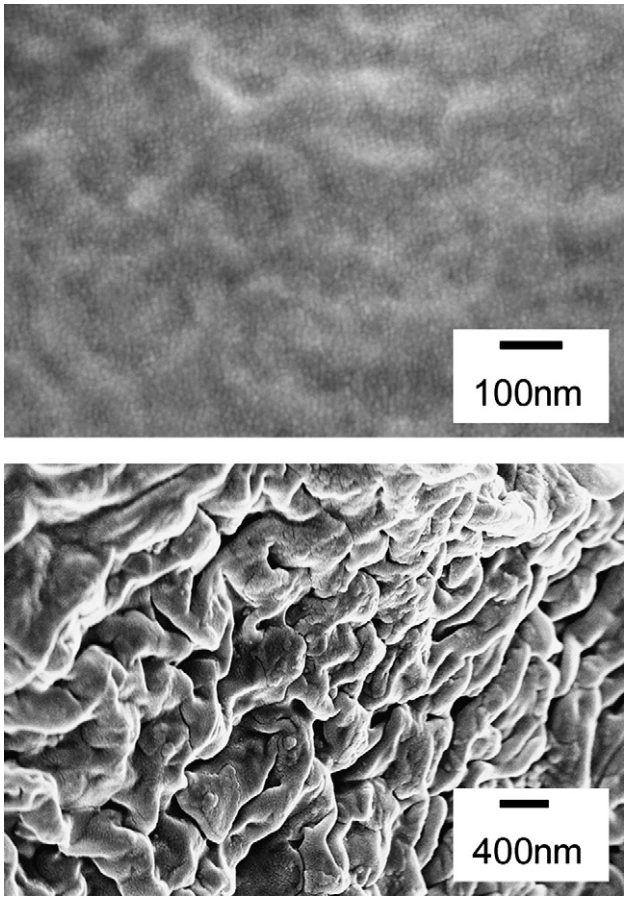

Fig. 4. SEM image of (i) A12M and (ii) A12MPOSS.

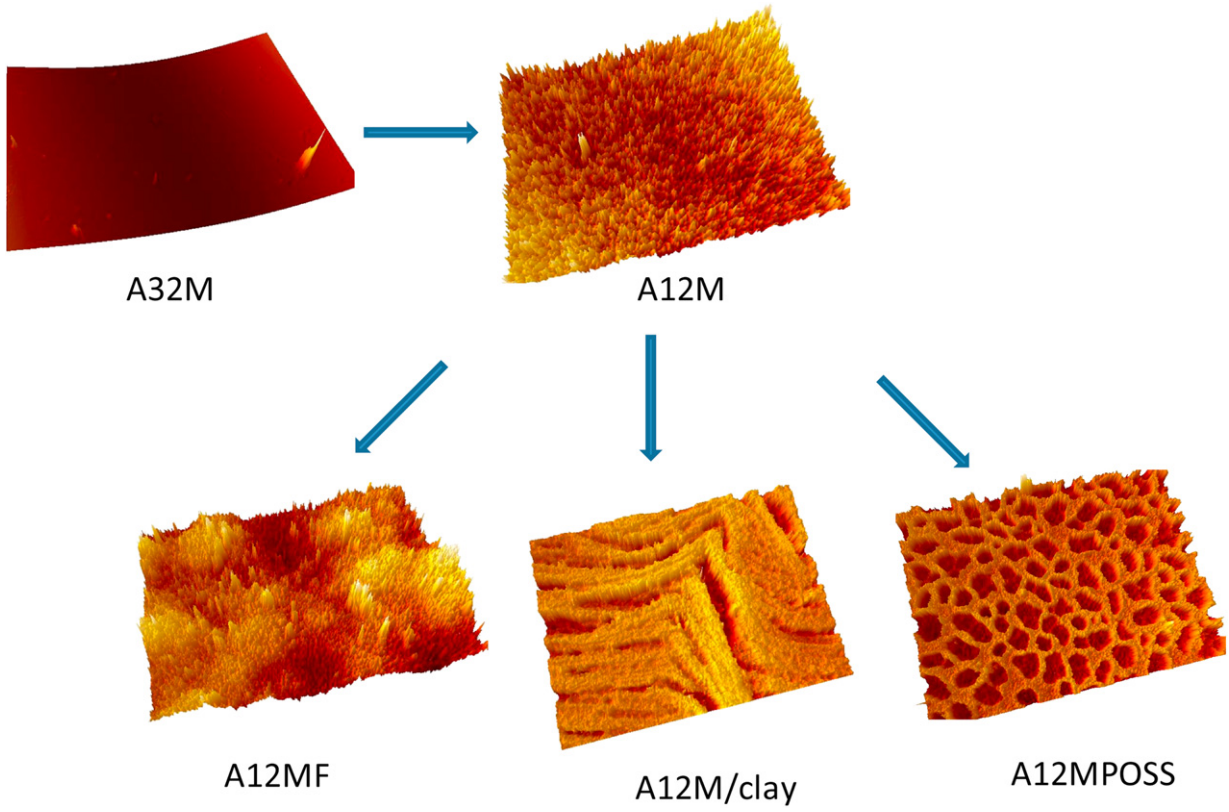

Fig. 5. 3-D profilometer images of solvent-casted samples: A32M (0.6 ± 0.2 μm), A12M (1.8 ± 0.3 μm), A12MF (5.3 ± 1.2 μm), A12M/clay (35 ± 6 μm), A12M/POSS (7 ± 0.8 μm) (scanned area 800×600 μm^2). For each sample, mean roughness and standard deviation are shown in parenthesis.

surface characterization is essential in order to gain some insight about the attachment/detachment mechanism.

XPS measurements were used to determine the actual surface atomic composition of the various systems in comparison to the stoichiometric (bulk) values (Fig. 3). The surface of the neat copolymer A12M is enriched with PDMS, as evidenced by the increased concentration of silicon and the reduced concentration of carbon (the stoichiometric ratio of carbon is higher for the hard segments). The fluorinated groups, covalently attached to the hard segments, compete with PDMS for surface migration, so that, overall, there is no accountable compositional deviation between the bulk and the surface in A12MF. Interpretation of the XPS data for A12MPOSS is not straightforward due to the compositional similarity between PDMS ($C_{30}H_{88}N_2O_{11}Si_{12}$) and POSS ($C_{33}H_{76}N_2O_{12}Si_8$). Nevertheless, SEM imaging of A12MPOSS surface (Fig. 4) reveal extensive migration of the low surface energy POSS nanoparticles to the surface, where they form large aggregates [37–39]. Similarly, the SEM image of the A12M surface also shows extensive phase segregation.

Interferometric profilometer images are shown in Fig. 5 and provide further insights to the surface organization of the various

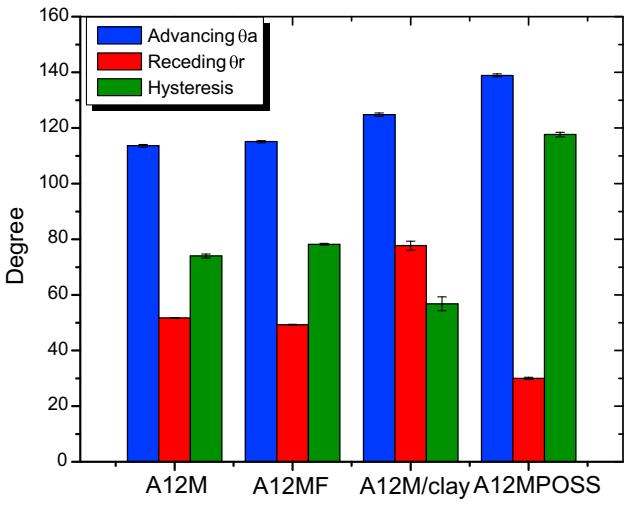

Fig. 6. Contact angle of different PDMS-polyurea segmented copolymer systems.

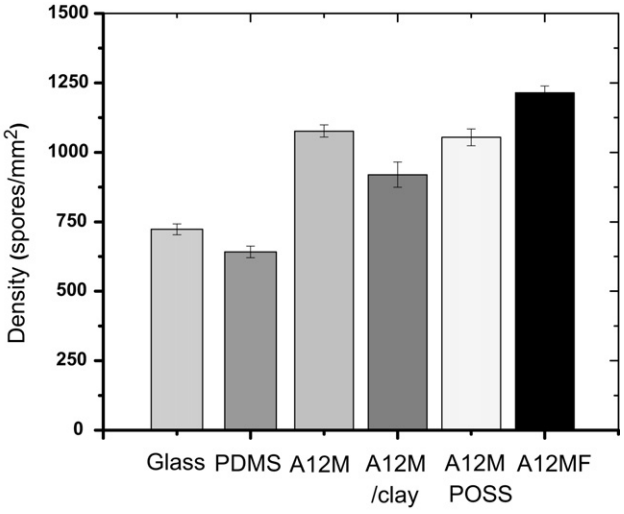

Fig. 7. Settlement density of *Ulva* spores on various PDMS-polyurea coatings.

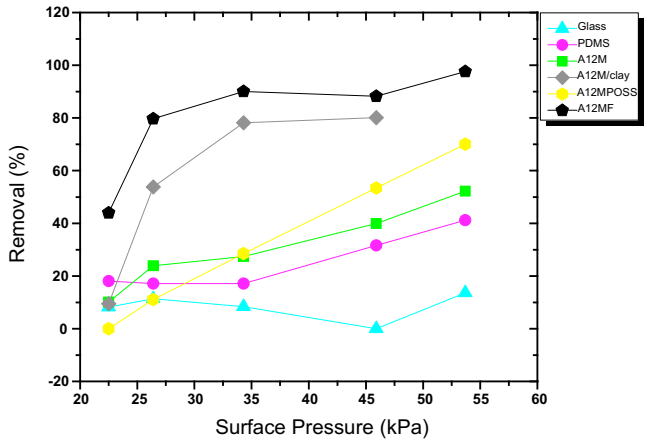

Fig. 8. Detachment of 7 day matured *Ulva* sporelings plotted as a function of water jet pressure (kPa).

systems. The topographic features of the surfaces mirror the chemical heterogeneity and the multiphase nature of the system. Only the A32M copolymer shows a smooth, uniform surface, in accordance to its minimal (1 wt%) hard segment content. In contrast, A12M (HSC = 12 wt%) posses a highly patterned yet rough surface that is characterized by a dense population of well resolved vertical features. Incorporation of fluorinated groups adds one more compositional variable that, in terms of surface topology, is translated to dual-scale roughness and asymmetric distribution of the irregular features. Turning to A12M/clay hybrid, the characteristic layered topographical pattern observed can be directly related to the platy geometry of the embedded nanoparticles. Lastly, the surface of the A12MPOSS is dominated by a continuous mosaic as a result of extensive nanoparticle clustering.

Further information about the surface of the coatings was obtained from contact angle measurements. The water advancing and receding contact angles (θ_a and θ_r, respectively) and the contact angle hysteresis, $\Delta\theta$ for the various surfaces were obtained using the Wilhelmy method [40]. For a given heterogeneous surface the values of these angles can deviate considerably from each other, since θ_a and θ_r correspond to the low and the high surface energy phase, respectively. Fig. 6 summarizes the contact angles measured for the various PDMS-polyurea based materials. The values measured should be compared to $\theta_a = 108^\circ$ reported for the standard PDMS homopolymer (namely Silastic^R-T2) [41]. Apparently, all systems considered display stronger hydrophobic characteristics compared to PDMS (greater θ_a), despite the presence of polar urea linkages to their molecular structure. This behavior might be related to the sparse density of urea linkages to the polymeric surface (as suggested by XPS), but it also reflects the inherent topographical complexity of the multiphase systems, as opposed to the homogeneous, one-phase PDMS elastomer. The high $\Delta\theta$ observed for all systems can be also attributed to the roughness of the surface [42,43]. In general, $\Delta\theta$ increases with surface roughness and reaches a maximum beyond which it drops rapidly [44]. Alternatively, large $\Delta\theta$ values have been attributed to an energy dissipation mechanism associated with thermodynamically irreversible molecular rearrangements on the solid surface that follows wetting [45–47]. A12MPOSS has both the highest θ_a and $\Delta\theta$ values (140 and 110° respectively), a behavior that has been previously reported for other POSS-containing hybrids [39].

Table 3
Critical surface pressure (P_{cr}) for 50% detachment of *Ulva* sporelings.

Surface	P_{cr}/kPa
A12MF	23
A12M/clay	26
A12MPOSS	44
A12M	52
PDMS	62 (extrapolated)
Glass	80 (extrapolated)

3.3. Biofouling testing

Tests using marine organisms confirmed the non-toxic character of the systems considered here. The settlement density of spores on various PDMS-polyurea based coatings is compared with a standard glass slide and a standard PDMS elastomer (Silastic^R-T2) in Fig. 7. All PDMS-polyurea based materials shows a higher spore settlement compared to neat PDMS, under identical experimental conditions. To a certain extent, this behavior can be due to the increased hydrophobicity of the copolymers compared to the homopolymer (as discussed above), given that even minor enhancements in hydrophobicity can accelerate the spore settlement considerably [48,49]. However, the data plotted in Fig. 7 do not support a simple correlation between the spore density of the various systems and the corresponding θ_a. This is not at all surprising since the attachment of biofoulants is a very complex procedure involving a variety of possible pathways that are case specific and extremely sensitive to the chemical composition, topography and wettability of the surface on one hand and the physiology of the living organism in a certain environment, on the other.

Fig. 8 shows the percent removal of sporelings from different PDMS-polyurea based coatings as a function of the applied pressure generated by a water jet. The corresponding pressures for 50% removal are listed in Table 3. All copolymer systems show better percent removal at pressures higher than 30 kPa. The A12MF coating shows enhanced release compared to PDMS at all pressures. The critical pressure for 50% removal, P_{cr}, is 60% lower for A12M/clay and A12MF compared to neat PDMS. Within the range of applied pressure, complete (100%) sporeling removal was achieved only from the A12MF coating. Recall that this surface is characterized by complex topography (Fig. 5). Enhanced fouling release performance has been attributed to increased surface lubricity that facilitates energy dissipation at localized levels through interfacial slippage [22,50]. Recall that the both advancing and receding angles for A12M and A12MF are very similar yet their fouling release behavior is very different. In our opinion fouling release seems to be dictated by topography and roughness that might impose steric constraints to the active contact area of biofoulants facilitating detachment.

Based on simple mechanics considerations the strength of adhesion of cylindrical objects attached to a smooth, homogenous surface is calculated to be proportional to the square root of the modulus of the substrate [51]. This relationship has been experimentally confirmed in detachment tests using marine organisms [13,52]. From an engineering perspective these results imply an inverse relationship between fouling release performance and mechanical strength of the coating, necessitating a compromise between those highly desirable properties. The present study suggests that this technological dilemma can be overcome through fine tuning of surface topography and chemical heterogeneity.

4. Conclusions

The extent of microphase separation, determined by the hard segment content, has a profound effect on the mechanical performance of PDMS-polyurea segmented copolymers. The thermomechanical properties can be further enhanced by incorporating

fluorinated or POSS-functionalized chain extenders or through nanoclay intercalation. The multiphase nature of the systems along with the great compositional diversity among them, give rise to a rich gallery of surface topological motifs. The surface topography can be tuned by controlling the microphase separation of the matrix and/or through nanoparticle incorporation. Bioadhesion to those nanostructured surfaces is determined by the interplay of roughness and wettability. The enhanced sporeling removal efficacy observed for each one of the materials considered here, coupled with their superior mechanical strength are attractive characteristics for potential fouling release applications. The present study provides further evidence that the technological dilemma between mechanical strength and fouling release performance can be resolved through fine tuning of the topographical characteristics of the surface of the coatings. It is also demonstrated that this design can be realized using easily synthesized and readily scalable coatings based on segmented PDMS-polyurea copolymers.

Acknowledgements

The work was supported by the Office of Naval Research. E. P. Giannelis acknowledges the support of Award No. KUS-C1-018-02, made by King Abdullah University of Science and Technology (KAUST). We acknowledge facility support through the Cornell Center for Materials Research (CCMR) and the Nanobiotechnology Center (NBTC).

References

[1] Omal I. Chemical Reviews 2003;103:3431–48.
[2] Railkin AI. Marine biofouling: colonization processes and defenses. CRC Press; 2004.
[3] Flemming HC, Sriyutha Murthy P, Venkatesan R, Cooksey KE. In: Marine and industrial biofouling. Springer; 2009.
[4] Townsin RL. Biofouling 2003;19:9–15.
[5] Schultz MP. Biofouling 2007;23:331–41.
[6] Geesey GG, Lewandowski Z, Flemming HC. In: Biofouling and biocorrosion in industrial water systems. CRC Press; 1994.
[7] Yebra DM, Kiil S, Kim DJ. Progress in Organic Coatings 2004;50:75–104.
[8] Kotrikla A. Journal of Environmental Management 2009;90:S77–85.
[9] Thomas KV, Brooks S. Biofouling 2010;26:73–88.
[10] Marechal JP, Hellio C. International Journal of Molecular Sciences 2009;10:4623–37.
[11] Krishman S, Welnman CJ, Ober CK. Journal of Materials Chemistry 2008;18:3405–13.
[12] Grozea CM, Walker GC. Soft Matter 2009;5:4088–100.
[13] Chaudhury MK, Finlay JA, Callow ME, Callow JA. Biofouling 2005;21:41–8.
[14] Stein J, Truby K, Wood C, Wendt DE, Smith J, Montemarano J, et al. Biofouling 2003;19:87–94.
[15] Schumacher JF, Carman ML, Callow ME, Callow JA, Finlay JA, Brennan AB. Biofouling 2007;23:55–62.
[16] Carman ML, Estes TG, Feinberg AW, Schumacher JF, Wilkerson W, Wilson LH, et al. Biofouling 2006;22:11–21.
[17] Schumacher JF, Aldred N, Callow ME, Finlay JA, Callow JA, Clare AS, et al. Biofouling 2007;23:307–17.
[18] Scardino AJ, Zhang H, Cookson DJ, Lamb RN, de Nys R. Biofouling 2009;25:757–67.
[19] Kim JH, Kim SH, Kim HK, Akaike T, Kim SC. Journal of Biomedical Materials Research 2002;62:613–21.
[20] Gudipati CS, Greenlief CM, Johnson JA. Journal of Polymer Science. Part A, Polymer Chemistry 2004;42:6193–208.
[21] Gudipati CS, Finlay JA, Callow JA, Callow ME, Wooley KL. Langmuir 2005;21:3044–53.
[22] Beigbeder A, Degeea P, Conlanb SL, Muttonb RJ, Clareb AS, Pettittc ME, et al. Biofouling 2008;24:291–302.
[23] Wouters M, Rentrop C, Willemsen P. Progress in Organic Coatings, in press.
[24] Sheth JP, Aneja A, Wilkes GL, Yilgor E, Atilla GE, Yilgor I, et al. Polymer 2004;45:6919–32.
[25] Bonart R, Muller EH. Journal of Macromolecular Science-Physics 1974; B10:177–89.
[26] Garrett JT, Runt J, Lin JS. Macromolecules 2000;33:6353–9.
[27] Choi T, Weksler J, Padsalgikar A, Runt J. Polymer 2009;50:2320–7.
[28] Abouzahr S, Wilkes GL, Ophir Z. Polymer 1982;23:1077–86.
[29] Wang CB, Cooper SL. Macromolecules 1983;16:775–86.
[30] Sarva SS, Hsieh AJ. Polymer 2009;50:3007–15.
[31] Clarson SJ, Dodgson K, Semlyen JA. Polymer 1985;26:930–4.
[32] Tan H, Guo M, Du R, Xie X, Li J, Zhong Y, et al. Polymer 2004;45:1647–57.
[33] Giannelis EP. Advanced Materials 1996;8:29–35.
[34] Crosby AJ, Lee JL. Polymer Reviews 2007;47:217–29. clay.
[35] Liff SM, Kumar N, McKinley GH. Nature Materials 2007;6:76–83.
[36] Liu H, Zheng S. Macromolecular Rapid Communications 2005;26:196–200.
[37] Koh K, Sugiyam S, Morinaga T, Ohno K, Tsuji Y, Fukuda T, et al. Macromolecules 2005;38:1264–70.
[38] Hosaka N, Torikai N, Otsuka H, Takahara A. Langmuir 2007;23:902–7.
[39] Misra R, Fu BX, Morgan SE. Journal of Polymer Science. Part B, Polymer Physics 2007;45:2441–55.
[40] Schmidt DL, DeKoven BM, Coburn CE, Potter GE, Meyers GF, Fischer DA. Langmuir 1996;12:518–29.
[41] Silver JH, Lin JC, Lim F, Tegoulia VA, Chaudhury MK, Cooper SL. Biomaterials 1999;20:1533–43.
[42] McHale G, Shirtcliffe NJ, Aqil S, Perry CC, Newton MI. Physical Review Letters 2004;93:036102–4.
[43] Quere D. Nature Materials 2002;1:14–5.
[44] Chau TT, Bruckard WJ, Koh PTL, Nguyen AV. Advances in Colloid and Interface Science 2009;150:106–15.
[45] Chen YL, Helm CA, Israelachvili JN. Journal of Physical Chemistry 1991;95:10736–47.
[46] Schmidt DL, Brady RF, Lam K, Schmidt DC, Chaudhury MJ. Langmuir 2004;20:2830–6.
[47] Martinelli E, Agostini S, Galli G, Chiellini E, Glisenti A, Pettitt ME, et al. Langmuir 2008;24:13138–47.
[48] Callow E, Callow JA, Ista LK, Coleman SE, Nolasco AC, Lopez GP. Applied and Environmental Microbiology 2000;66:3249–54.
[49] Ista LK, Callow ME, Finlay JA, Coleman SE, Nolasco AC, Simons RH, et al. Environmental Microbiology 2004;70:4151–7.
[50] Newby B-M, Chaudhury MK. Langmuir 1997;13:1805–9.
[51] Brady RF. Progress in Organic Coatings 2001;43:188–92.
[52] Brady RF. Progress in Organic Coatings 1999;35:31–5.